Journal of Molecular Liquids 302 (2020) 112518

Contents lists available at ScienceDirect

Journal of Molecular Liquids

journal homepage: www.elsevier.com/locate/molliq

Viscosity of 2-ethylhexan-1-amine (EHA)-diglyme, EHA-triglyme and EHA-tetraglyme non-aqueous solutions and its effect on initial absorption rate

Kun Fu, Pan Zhang, Lemeng Wang, Xiayu Huang, Dong Fu *

Hebei Key Lab of Power Plant Flue Gas Multi-Pollutants Control, Department of Environmental Science and Engineering, North China Electric Power University, Baoding 071003, People's Republic of China

ARTICLE INFO

Article history:
Received 1 October 2019
Received in revised form 10 January 2020
Accepted 16 January 2020
Available online 20 January 2020

Keywords:
Viscosity
CO_2
EHA
Ether
Non-aqueous absorbent
Initial absorption rate

ABSTRACT

The viscosities (η) of 2-ethylhexan-1-amine (EHA), diglyme, triglyme, tetraglyme and EHA-diglyme/triglyme/tetraglyme non-aqueous solutions were measured by using the NDJ-5S rotational viscometer at 101 kPa. The temperatures (T) ranged from 303.2 K to 323.2 K. The mass fractions of EHA (w_{EHA}) ranged from 0.100 to 0.900. The viscosity was modeled and the calculated results agreed well with the experiments. The effects of w_{EHA} and T on viscosity were demonstrated on the basis of experiments and calculations. The initial absorption rates of CO_2 (r) in EHA-diglyme/triglyme/tetraglyme non-aqueous solutions were measured, and the effects of viscosity, absorbent concentration and absorption rate constant of CO_2 (k) on initial absorption rates were demonstrated. Our research shows that in the temperature range of 303.2 K to 323.2 K, the proposed three non-aqueous absorbents have small solution viscosities (<3 mPa·s), which is beneficial to the mass transfer of CO_2 absorption and the initial absorption rate. Thus the proposed non-aqueous absorbents have good application potential in the field of CO_2 capture process.

© 2020 Elsevier B.V. All rights reserved.

1. Introduction

In the past decades, greenhouse gas like carbon dioxide (CO_2) has increasingly released into the atmosphere, resulting in critical global warming, which may cause severe environmental issues including climate change, extreme weather and the rise of sea level [1,2]. The reduction of CO_2 plays an important role in global sustainable development. In recent years, CO_2 capture demonstration projects have been launched in various countries around the world. Especially in China, CO_2 capture from thermal power plants has achieved significant results and caused widespread concern [3–5].

Generally, CO_2 emissions from thermal power plants can be removed by many methods including absorption, adsorption and membrane [6]. Among these methods, chemical absorption using alkanolamine aqueous solutions as absorbents is one of the most popular and feasible approaches because CO_2 can be satisfactorily removed and the absorbent is expected to be well regenerated by heating [7]. However, most of the conventional amine absorbents are of solvent water-based absorbents, which contain a significant amount of water as solvent and suffer from serious downsides such as strong steel corrosivity and enormous energy consumption in rich solution regeneration and lean solution cooling [8–10].

In recent years, non-aqueous alkanolamine solutions have attracted much attention for CO_2 capture [11–14]. Compared with the solvent water-based CO_2 absorption process, the water-lean or non-aqueous absorption process replaces part or all of the solvent water with an organic solvent or functional ionic liquid. It may effectively lessen the thermal degradation, reduce the latent heat of evaporation in the regeneration process and greatly reduce the total energy consumption [15–17]. Moreover, equipment corrosion may be minimized because of the absence of water [18,19]. Fu et al. [20] showed that MEA-methanol non-aqueous solution had a higher overall gas-phase mass transfer coefficient (K_Ga_v) than MEA aqueous solution at low CO_2 partial pressure. Kang et al. [21] revealed that MEA-ethylene glycol (EG) non-aqueous absorbents were superior to conventional water-based ones, exhibiting higher CO_2 absorption capacity and lower regeneration energy consumptions. Zheng et al. [22] concluded that compared to AMP aqueous solution, AMP-EG non-aqueous solution had a higher circular loading of CO_2, especially at lower desorption temperature. The mixture of ionic liquids with MDEA has also drawn attention, e.g., Xiao et al. [23] proved that the MDEA-1-butyl-3-ethylimidazolium tetrafluoroborate

* Corresponding author at: Department of Environmental Science and Engineering, North China Electric Power University, Baoding 071003, People's Republic of China.
E-mail address: fudong@tsinghua.org.cn (D. Fu).

https://doi.org/10.1016/j.molliq.2020.112518
0167-7322/© 2020 Elsevier B.V. All rights reserved.

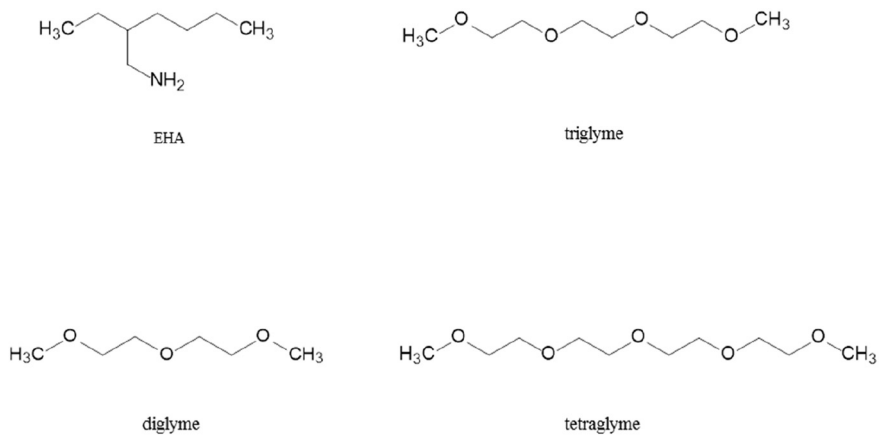

Fig. 1. Structures of EHA, diglyme, triglyme and tetraglyme.

non-aqueous system led to high cycling CO_2 capacity, energy-saving and good regenerability.

However, it is worth noting that the use of high volatile alcohols as solvent seems to cause a heavy solvent loss in industrial applications [24,25]. Moreover, in the case of high-water depletion, the viscosity of the absorbent containing low volatile glycols or functional ionic liquids may dramatically increase, thus has a significant impact on the absorption rate and mass transfer coefficient [26,27]. Therefore, it is of great significance to select solvents with low volatility and low viscosity. Some literatures showed that polyethylene glycol ethers such as diglyme, triglyme and tetraglyme take the advantages of high boiling point, low volatility and low viscosity [28,29]. Besides, 2-ethylhexan-1-amine (EHA) is a sterically hindered primary alkanolamine, and does not form a precipitate when it reacts with CO_2 in polyethylene glycol ethers [30]. Accordingly, we proposed three blends containing EHA and polyethylene glycol ethers (EHA-diglyme/triglyme/tetraglyme) as non-aqueous absorbents to capture CO_2. As viscosity data are required when designing or simulating absorption and regeneration columns for CO_2 capture using these non-aqueous absorbents, it is necessary to study the quantitative relationship between viscosity and operating conditions such as mass fraction and temperature [31–34]. Kodamaa et al. [29] measured the viscosities of diglyme, triglyme and tetraglyme between 273.15 K and 363.15 K at atmospheric pressure. However, the experimental and theoretical work for the viscosities of EHA and EHA-diglyme/triglyme/tetraglyme non-aqueous solutions has been rarely reported so far.

The main purpose of this work is to investigate the viscosities of EHA-ether non- aqueous solutions experimentally and theoretically, and then demonstrate the effects of mass fraction of EHA (w_{EHA}) and temperature (T) on the viscosity, and the effects of w_{EHA} and viscosity on the initial absorption rate (r). To this end, the viscosities of EHA, diglyme, triglyme, tetraglyme and EHA-diglyme/triglyme/tetraglyme non-aqueous solutions were measured by using the NDJ-5S rotational viscometer, with w_{EHA} and T ranging from 0.100 to 0.900 and 303.2 K to 323.2 K respectively. Besides experiments, the Weiland equation [35] was used to model the viscosities and their mass fraction and temperature dependences. The viscosities and CO_2 initial absorption rates of non-aqueous absorbents and some solvent water-based absorbents were compared, and the factors influencing the initial absorption rate were discussed.

2. Experimental

2.1. Materials

The samples used in this work are detailed in Table A.1 and Fig. 1. They were used without further purification. As shown in Fig. 1, the amino group accompanied by a steric hindrance on the molecular

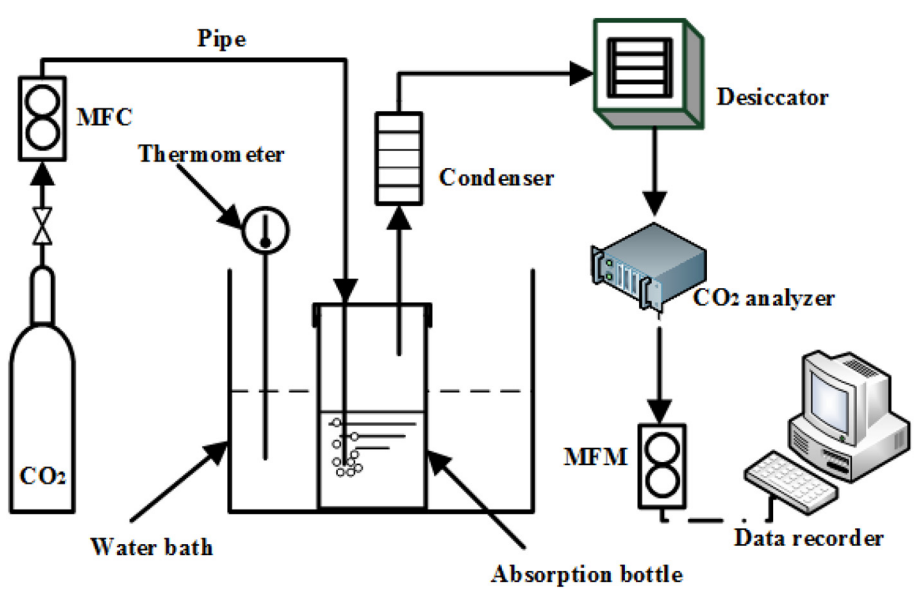

Fig. 2. Schematic diagram for absorption capacity measurement.

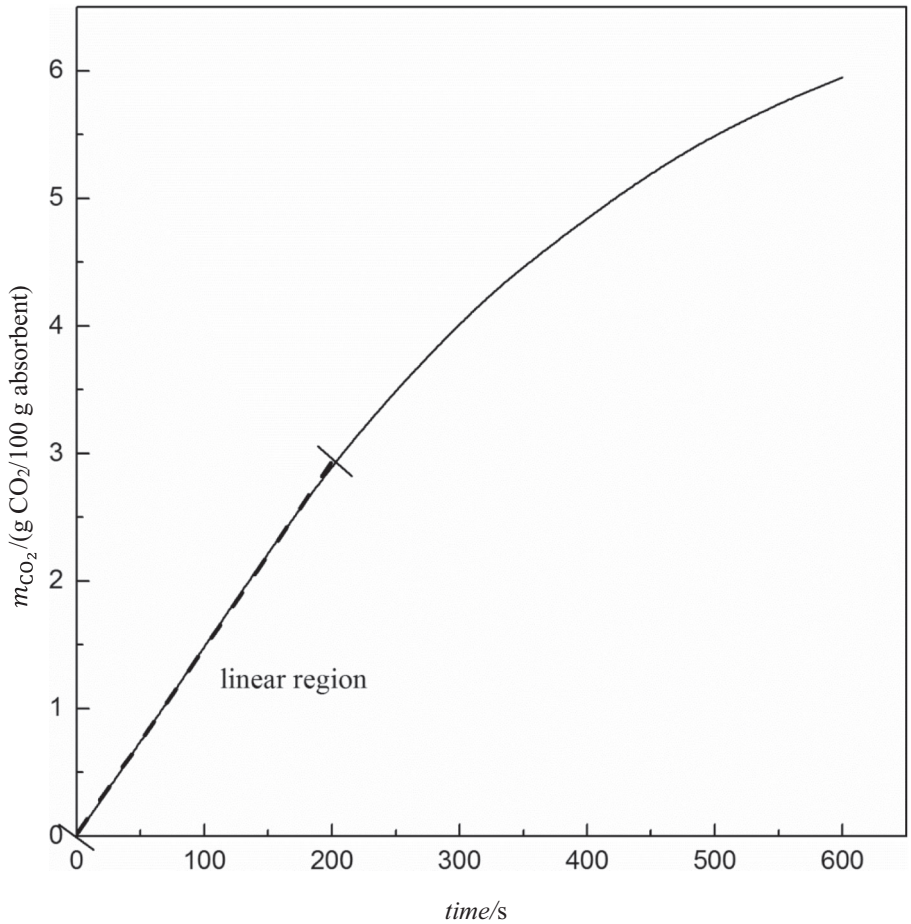

Fig. 3. Time dependence of the mass of absorbed CO_2 for 30 wt%EHA-70 wt%tetraglyme non-aqueous absorbent. $T = 313.2$ K. The black dashed line shows the linear region used to calculate the initial absorption rate of CO_2.

structure enables EHA to have a good ability to absorb CO_2, and form instable carbamate [36,37]. The ether groups on the molecular structure enable diglyme, triglyme and tetraglyme to have good solubility to the carbamate, which makes the regeneration temperature of carbonated EHA-ether system expected to be <373 K [9,30]. Moreover, the boiling points of diglyme, triglyme and tetraglyme are 435 K, 489 K and 548 K, respectively. Thus, during the regeneration process, heat consumption and mass loss from the solvent evaporation should be much less than those of water-based absorbents like MEA aqueous solution.

An analytical balance (FA1604A, manufactured by Shanghai Jingtian Electronic Instrument Co., Ltd., uncertainty = 0.2 mg at a 95% confidence level) was used to weigh all the required samples. Taking the purity into account, the uncertainties of w_{EHA}, $w_{diglyme}$, $w_{triglyme}$ and $w_{tetraglyme}$ are respectively estimated as 0.024, 0.012, 0.024 and 0.024 at a 95% confidence level.

2.2. Apparatus and procedures

The viscosities of EHA, diglyme, triglyme, tetraglyme and EHA-diglyme/triglyme/tetraglyme non-aqueous solutions were measured from 303.2 K to 323.2 K by using the NDJ-5S digital rotational viscometer (uncertainty = 2% at a 95% confidence level) thermostated with a circulating constant temperature water bath (uncertainty = 0.2 K at a 95% confidence level). The viscometer was designed and built with five cylindrical rotors (0#, 1#, 2#, 3# and 4#) and four different velocities (6 rpm, 12 rpm, 30 rpm and 60 rpm). In this work, the selected combination of rotor and rotating speed was 0#-60 rpm, which corresponded to the upper limit of 10 mPa·s.

To measure the initial absorption rates of CO_2, we firstly need to determine the mass of absorbed CO_2 in a certain amount of absorbent. The schematic diagram for absorption capacity measurement is shown in

Table 1
Comparisons between the experimental values (η_{exp}) and certified values (η_{cer}), and the average relative deviation (ARD) between η_{exp} and η_{cer}. Pressure (p) = 101 kPa.

Number	η/(mPa·s)[a]					
	303.2 K		313.2 K		323.2 K	
	η_{exp}	η_{cer}	η_{exp}	η_{cer}	η_{exp}	η_{cer}
GBW(E)130611	1.34	1.379	1.15	1.171	0.98	1.006
GBW(E)130612	3.14	3.126	2.49	2.487	2.03	2.026
GBW(E)130613	5.82	5.846	4.40	4.416	3.43	3.447
	ARD = 1.03%[b]					

[a] Expanded uncertainties U at a 95% confidence level are $U_{95}(T) = 0.2$ K; $U_{95}(p) = 4$ kPa; $U_{r,95}(\eta_{exp}) = 2\%$; $U_{r,95}(\eta_{cer}) = 0.4\%$. $U_{r,95}(\eta_{cer})$ was stated by the supplier.
[b] ARD = $\sum_{i=1}^{9} \left| 1-\frac{\eta_{exp}}{\eta_{cer}} \right| / 9 \times 100\%$.

Table 2
Viscosities of EHA, diglyme, triglyme and tetraglyme from this work (η_{exp})[a] and Ref. [29] (η_{ref}), and the corresponding average relative deviation (ARD) between η_{exp} and η_{ref}. Pressure (p) = 101 kPa.

Sample	η/(mPa·s)					
	303.2 K		313.2 K		323.2 K	
	η_{exp}	η_{ref}	η_{exp}	η_{ref}	η_{exp}	η_{ref}
EHA	0.98		0.85		0.74	
diglym	0.95	0.901	0.81	0.777	0.69	0.676
triglyme	1.83	1.78	1.54	1.48	1.31	1.25
tetraglyme	3.06	2.99	2.52	2.45	2.10	2.02
	ARD = 3.62%[b]					

[a] Expanded uncertainties U at a 95% confidence level are $U_{95}(T) = 0.2$ K; $U_{95}(p) = 4$ kPa; $U_{r,95}(\eta) = 2\%$.
[b] ARD $= \sum_{i=1}^{9} \left| 1-\frac{\eta_{exp}}{\eta_{ref}} \right| /9 \times 100\%$.

Fig. 2. The details have been described in our previous work [38,39]. When the mass of the absorbed CO_2 is obtained, the initial absorption rates of CO_2 (g CO_2/100 g absorbent/s) were calculated from the linear regression (R^2>0.995) of the slope of the time-dependent absorption capacity curve [40]. We found the R^2 values were >0.995 in the first 200 s for all the non-aqueous absorbents ($w_{EHA} \geq 0.300$) investigated in this work. The linear regression for 30 wt%EHA-70 wt%tetraglyme non-aqueous absorbent is shown in Fig. 3.

3. Results and discussion

3.1. Viscosity

To verify the reliability of the experimental apparatus, the viscosities of three viscosity standard liquids were measured at 303.2 K, 313.2 K and 323.2 K. Table 1 shows the comparisons between the experimental values from this work (η_{exp}) and those certified by Chinese National Institute of Metrology (η_{cer}) [41–43]. The average relative deviation (ARD) between η_{exp} and η_{cer} is 1.03%, indicating that the apparatus is reliable.

Table 2 shows the comparison of the viscosities of three ethers from this work (η_{exp}) and from Ref. [29] (η_{ref}). The water contents (mass percent) of diglyme, triglyme and tetraglyme used in this work (purity ≥99 wt%) are respectively 0.4%, 0.0036% and 0.03% (determined by using the Karl Fischer method, as stated by the supplier). The three ethers (purity ≥99 wt%) used in Ref. [29] were dried with a Molecular Sieve 4A and percolated through a glass filter in a globe box filled with dry Ar [29]. The ARD between η_{exp} and η_{ref} is 3.62%. One may find from Table 2 and Fig. 4 that the viscosities decrease with increasing temperature. Moreover, the comparison shows that the viscosity of EHA is slightly higher than that of diglyme, yet significantly lower than those

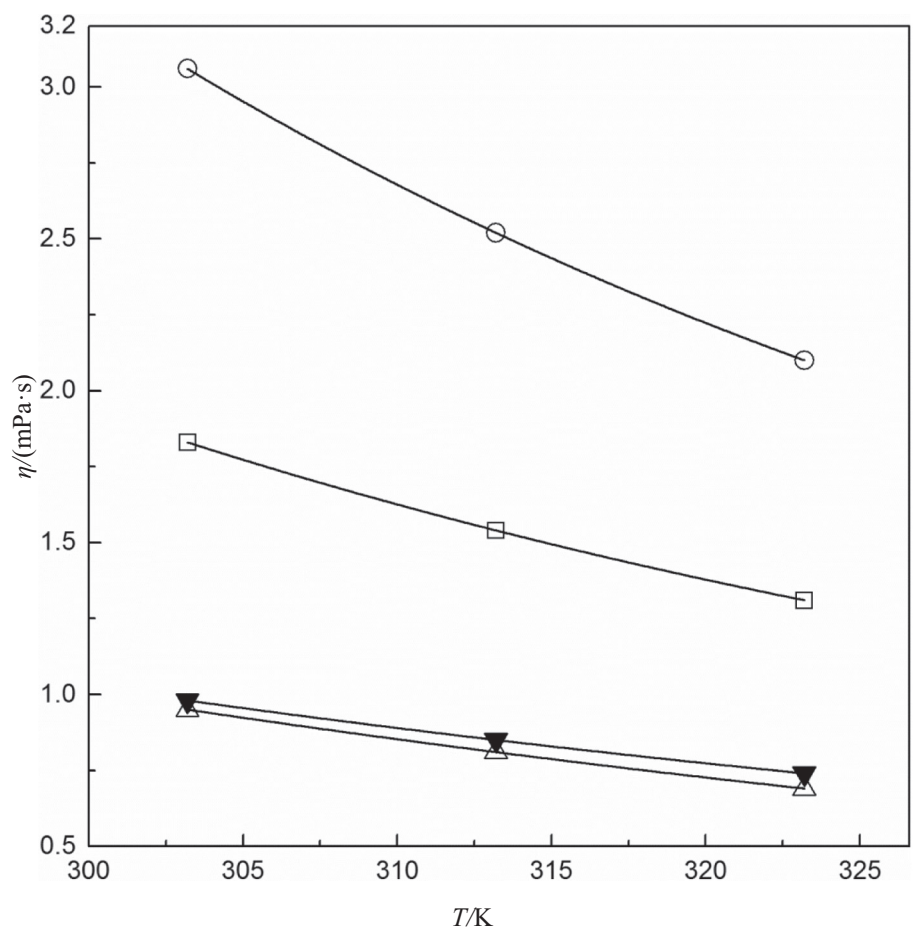

Fig. 4. Temperature dependence of the viscosities of EHA (▼), diglyme (△), triglyme (□) and tetraglyme (○). Symbols: experimental values from this work. Lines: trend lines.

of triglyme and tetraglyme at a given temperature, e.g., in the case of $T = 313.2$ K, the viscosities of EHA, diglyme, triglyme and tetraglyme are 0.85 mPa·s, 0.81 mPa·s, 1.54 mPa·s and 2.52 mPa·s, respectively.

The experimental results of the viscosities of EHA-diglyme/triglyme/tetraglyme non-aqueous solutions are shown in Table 3. Besides experiments, equations those can correctly correlate viscosities are also important. According to the work of Weiland et al. [35]. The viscosity of amine-water binary system can be calculated from:

$$\eta_i = \eta_{water} \times \exp\left\{\frac{[(a_i\Omega + b_i)T + (c_i\Omega + d_i)]\Omega}{T^2}\right\} \quad (1)$$

where η_i and η_{water} are the viscosities of the amine solution and water respectively (mPa·s), Ω is the mass percent of amine, a_i, b_i, c_i, d_i are adjustable parameters.

In this work, the solvent water was replaced with ether. Thus, the viscosity of EHA-ether binary system may be calculated from:

$$\eta_i = \eta_{ether} \times \exp\left\{\frac{[(a_i\Omega + b_i)T + (c_i\Omega + d_i)]\Omega}{T^2}\right\} \quad (2)$$

where η_{ether} is the viscosity of ether.

The model parameters of EHA-diglyme/triglyme/tetraglyme non-aqueous solutions, a_i, b_i, c_i, d_i were regressed by fitting to the experimental data of the corresponding binary system. The objective function (ARD) is expressed as:

$$fs = \sum_{i=1}^{n}\left|1 - \eta_{cal}/\eta_{exp}\right|/n \times 100\% \quad (3)$$

Table 3
Viscosities (η) of EHA-diglyme/triglyme/tetraglyme non-aqueous solutions under different mass fractions of EHA (w_{EHA}) and temperatures (T). Pressure (p) = 101 kPa.[a]

w_{EHA}	w_{ether}	η/(mPa·s)		
		303.2 K	313.2 K	323.2 K
$w_{diglyme}$				
0.100	0.900	0.94	0.81	0.70
0.200	0.800	0.93	0.80	0.69
0.300	0.700	0.92	0.79	0.68
0.400	0.600	0.93	0.80	0.69
0.500	0.500	0.94	0.81	0.70
0.600	0.400	0.95	0.82	0.71
0.700	0.300	0.96	0.84	0.73
0.800	0.200	0.97	0.85	0.74
0.900	0.100	0.98	0.86	0.75
$w_{triglyme}$				
0.100	0.900	1.64	1.39	1.20
0.200	0.800	1.54	1.31	1.13
0.300	0.700	1.39	1.16	1.00
0.400	0.600	1.32	1.11	0.95
0.500	0.500	1.25	1.06	0.91
0.600	0.400	1.19	1.01	0.88
0.700	0.300	1.13	0.97	0.84
0.800	0.200	1.05	0.90	0.79
0.900	0.100	1.02	0.88	0.76
$w_{tetraglyme}$				
0.100	0.900	2.55	2.09	1.76
0.200	0.800	2.24	1.87	1.58
0.300	0.700	1.99	1.59	1.35
0.400	0.600	1.74	1.43	1.22
0.500	0.500	1.58	1.30	1.11
0.600	0.400	1.39	1.16	1.00
0.700	0.300	1.26	1.07	0.92
0.800	0.200	1.14	0.97	0.84
0.900	0.100	1.04	0.89	0.78

[a] Expanded uncertainties U at a 95% confidence level are $U_{95}(T) = 0.2$ K; $U_{95}(p) = 4$ kPa; $U_{95}(w_{EHA}) = 0.024$; $U_{95}(w_{diglyme}) = 0.012$; $U_{95}(w_{triglyme}) = 0.024$; $U_{95}(w_{tetraglyme}) = 0.024$; $U_{r,95}(\eta) = 2\%$.

where the subscripts 'cal' and 'exp' stand for the calculated and experimental data respectively, and n is the number of data.

Using the experimental data presented in Table 3 and Eqs. (2) and (3), the optimized model parameters and the corresponding ARD determined for three EHA-ether non-aqueous solutions are listed in Table 4. The ARD for EHA-diglyme, EHA-triglyme, EHA-tetraglyme non-aqueous solutions are 0.77%, 1.25% and 1.34%, respectively, indicating that the results are satisfactory. The agreement of the correlation is shown in Fig. 5, in which the solid diagonal line demonstrates the hypothetical exact fit. The insert plot in Fig. 5 shows the deviations between experimental and calculated data. The maximum and minimum deviations are −4.14% and 0 respectively. Fig. 5 implies that there is good compatibility between experimental and calculated values, thus the presented model correctly captures the mass fraction and temperature dependences of the viscosities of EHA-diglyme/triglyme/tetraglyme non-aqueous solutions.

Figs. 6, 7 and 8 show the influence of mass fraction of EHA and temperature on the viscosities of EHA-diglyme, EHA-triglyme and EHA-tetraglyme non-aqueous solutions, respectively. One finds from the insert plots of these figures that the effect of temperature on viscosity is relatively simple. For the three non-aqueous solutions, under certain conditions, their viscosity monotonously decreases with the increase of temperature. Compared with the effect of temperature, the effect of solution composition (especially w_{EHA}) on viscosity is much more complicated.

For EHA-diglyme non-aqueous solution, when w_{EHA} changed from 0.100 up to 0.900, the solution viscosity decreased slightly at first, reached a minimum value, and then began to increase, however, for EHA-triglyme and EHA-tetraglyme non-aqueous solutions, the viscosity decreased monotonously in the EHA concentration range of 0.100 to 0.900. In general, in a multicomponent aqueous solution, with the increase of solute mass fraction, it is often observed that the solution viscosity increases at first, reaches a maximum value and then decreases, and such phenomenon can be explained by the hydrophobic effect of solute [44]. However, in this work, EHA and diglyme are both organics, thus there is no solute hydrophobic effect on solution viscosity. The minimum viscosity of EHA-diglyme non-aqueous solution appears near w_{EHA} of 0.300, and the minimum value is not significant. We believe the main reason is that the viscosity values of pure EHA and pure diglyme are relatively close, and the excess viscosity ($\eta^{ex} = \eta_{exp}$-$x_1\eta_1$- $x_2\eta_2$, here x is the mole fraction, subscript 1 and 2 refer to EHA and diglyme, respectively) during the mixing process is very small. We found at 303.2 K, 313.2 K and 323.2 K, all the minimum η^{ex} (−0.039 mPa·s, −0.032 mPa·s, and −0.025 mPa·s) appeared at w_{EHA} around 0.300. For EHA-triglyme and EHA-tetraglyme non-aqueous solutions, as the viscosity of pure EHA is much lower than the viscosities of pure triglyme and pure tetraglyme, the viscosity decreases significantly with increasing w_{EHA}. Moreover, as the viscosity of pure tetraglyme is larger than that of pure triglyme, the viscosity of EHA-tetraglyme non-aqueous solution decreases much faster than that of EHA-triglyme non-aqueous solution.

3.2. The initial absorption rate of CO_2

The absorption of CO_2 in absorbent B may be formulated as [45]:

$$N \propto C_A a\sqrt{kC_B D_A} \quad (4)$$

Table 4
Model parameters and the corresponding average relative deviation (ARD) between calculations and experiments.

Non-aqueous solution	Model parameters				ARD
	a_i	b_i	c_i	d_i	
EHA-diglyme	0.0459	0.1960	−12.0032	−189.0307	0.77%
EHA-triglyme	0.0136	−2.8348	−1.2385	2.6235	1.25%
EHA-tetraglyme	0.0340	−5.0732	−5.5828	12.0401	1.34%

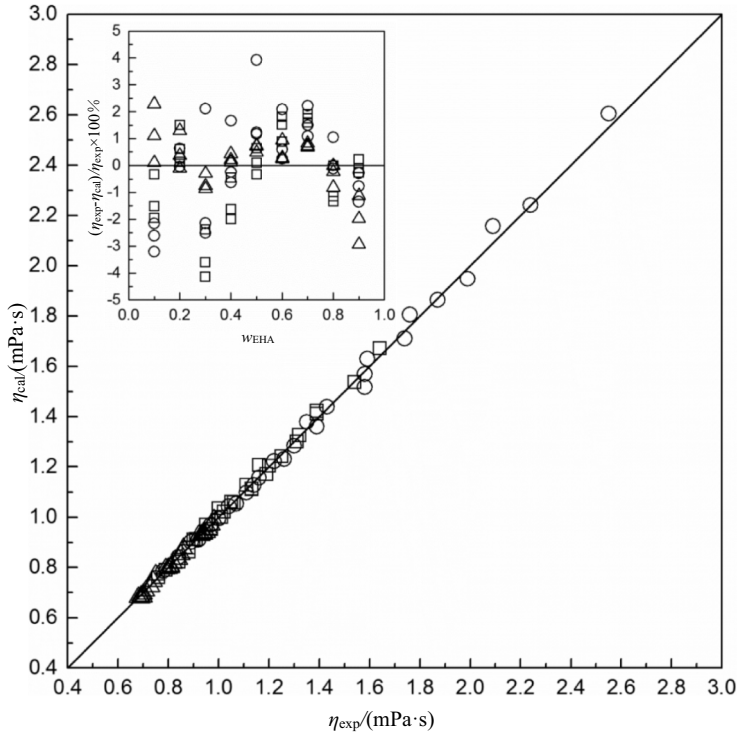

Fig. 5. Comparisons of the experimental viscosity (η_{exp}) with the calculated viscosity (η_{cal}). Main plot: comparisons of experimental and calculated state variables. Insert plot: normalized deviation plot for the viscosities of the three EHA-ether non-aqueous solutions. Symbols: △EHA-diglyme; □EHA-triglyme; ○EHA-tetraglyme.

where N is the absorption rate, C_A is the concentration of CO_2, a is the absorbing surface area, k is the absorption rate constant, C_B is the concentration of the effective absorbent. D_A is the diffusion coefficient of gas in liquid phase, which is dominated by the viscosity of the absorbent, and can be estimated as [46]:

$$D_A = \left(14 \times 10^{-5}\right) / \left[\eta_{water}(1.1 \times L_a/L_w)V_m^{0.6}\eta\right] \quad (5)$$

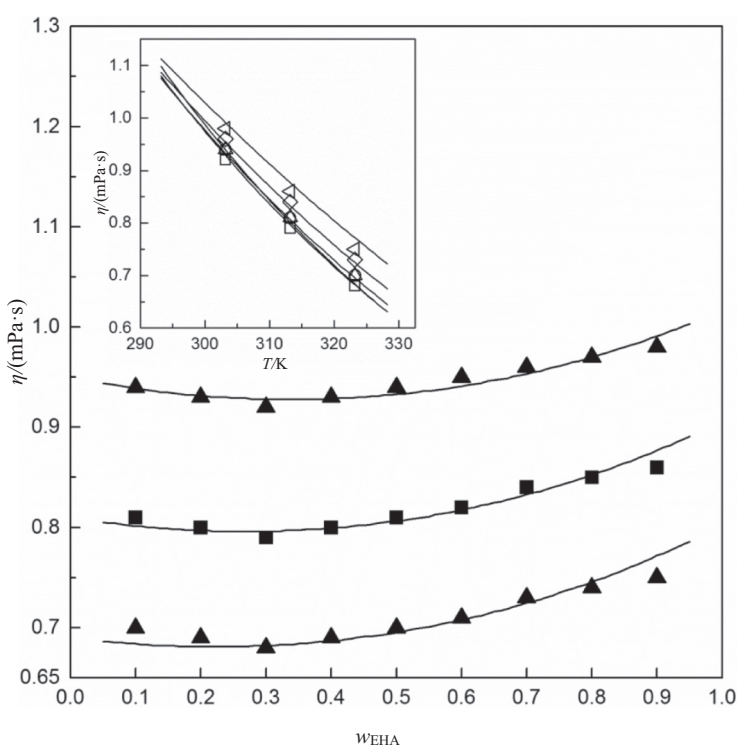

Fig. 6. w_{EHA} and temperature (insert plot) dependences of the viscosities of EHA-diglyme non-aqueous solutions. Symbols: experimental values from this work. Main plot: ▲T = 303.2 K; ■T = 313.2 K; ●T = 323.2 K. Insert plot: △w_{EHA} = 0.1; □w_{EHA} = 0.3; ○w_{EHA} = 0.5; ◇w_{EHA} = 0.7; ◁w_{EHA} = 0.9. Lines: calculated values from this work.

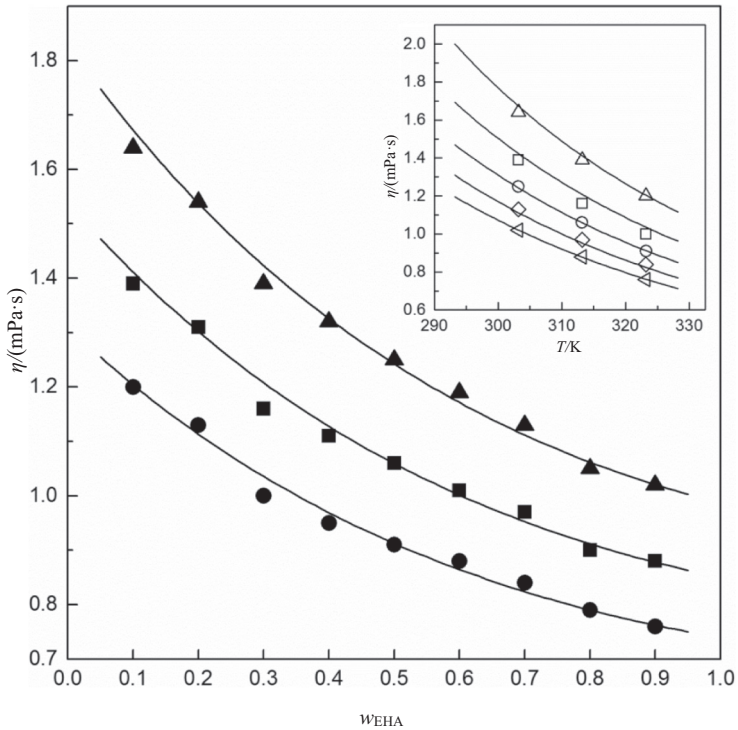

Fig. 7. w_{EHA} and temperature (insert plot) dependences of the viscosities of EHA-triglyme non-aqueous solutions. Symbols: experimental values from this work. Main plot: ▲$T = 303.2$ K; ■$T = 313.2$ K; ●$T = 323.2$ K. Insert plot: △$w_{EHA} = 0.1$; □$w_{EHA} = 0.3$; ○$w_{EHA} = 0.5$; ◇$w_{EHA} = 0.7$; ◁$w_{EHA} = 0.9$. Lines: calculated values from this work.

where η_{water} is the viscosity of water, L_a and L_w are the latent heat of evaporation of the absorbent and water respectively, V_m is the molar volume of diffusing substance, η is the viscosity of the absorbent which can be expressed by using Eqs. (1) and (2). Combining Eqs. (4) and (5) gives:

$$N \propto (kC_B/\eta)^{0.5} \tag{6}$$

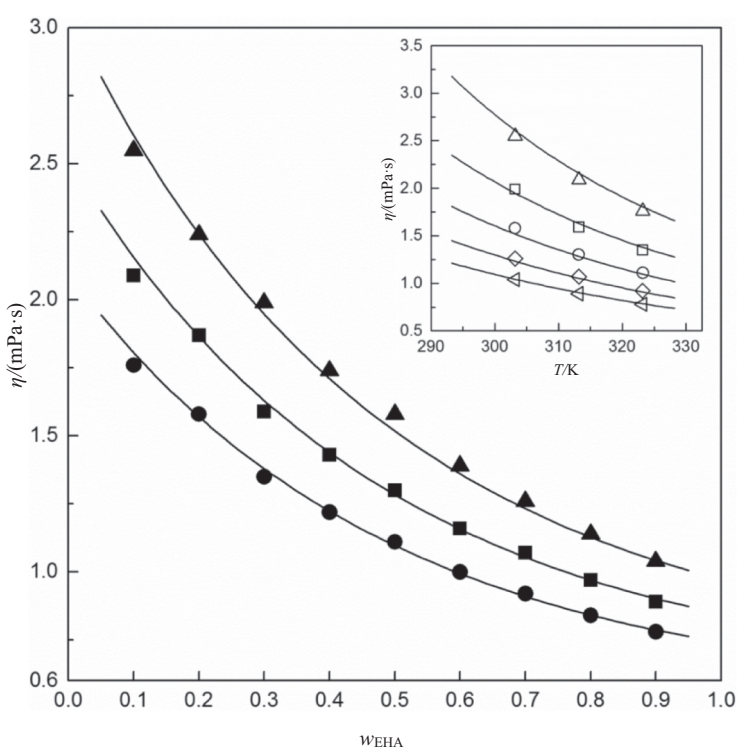

Fig. 8. w_{EHA} and temperature (insert plot) dependences of the viscosities of EHA-tetraglyme non-aqueous solutions. Symbols: experimental values from this work. Main plot: ▲$T = 303.2$ K; ■$T = 313.2$ K; ●$T = 323.2$ K. Insert plot: △$w_{EHA} = 0.1$; □$w_{EHA} = 0.3$; ○$w_{EHA} = 0.5$; ◇$w_{EHA} = 0.7$; $w_{EHA} = 0.9$. Lines: ◁calculated values from this work.

It can be seen from Eq. (6) that either a lower viscosity or a higher concentration of the absorbent may lead to a higher absorption rate.

In order to demonstrate the competitive effects of the solution viscosity and solution mass fraction on the absorption performance of CO_2 in absorbents, in our previous work, we have measured and calculated the viscosities of many water-based absorbents with promising application potential in industrial CO_2 capture process, in particular, the viscosities of blended alkanolamine-amino acid ionic liquid (AAIL) aqueous solutions [47,48]. We found that when the mass fraction of absorbent is higher than 50 wt% (water content <50 wt%), the solution viscosity may seriously impede the CO_2 absorption. Thus, when a blended alkanolamine-AAIL aqueous solution is used as CO_2 absorbent, the mass fraction of the effective absorbent is generally lower than 50 wt% in order to ensure a satisfactory absorption rate, but in this case, a lot of wasted effort must be consumed in the processes of the rich solution regeneration and lean solution cooling.

In this work, we measured the initial absorption rates of CO_2 in EHA-diglyme/triglyme/tetraglyme non-aqueous solutions at 313.2 K and 101 kPa, and then compared these data with those of blended alkanolamine-AAIL aqueous solutions (including MDEA-tetramethylammonium glycinate/[N_{1111}][Gly] and MDEA-1-butyl-3-methylimidazolium lysinate/[Bmim][Lys]), as shown in Table 5.

One finds from Table 5 that the viscosities of EHA-diglyme/triglyme/tetraglyme non-aqueous solutions are much lower than those of alkanolamine-AAIL aqueous solutions. Correspondingly, the initial absorption rates in the former three non-aqueous solutions are three to five times higher than those in the latter aqueous solutions, indicating that a relatively low viscosity is conducive to the increase of initial absorption rate. One may also find from this table that in the three non-aqueous solutions, all the effective absorbent concentrations are 50 wt %, yet the initial absorption rate does not change monotonously with increasing viscosity, indicating that the initial absorption rate is not only related to viscosity and absorbent concentration, but also to the absorption rate constant of CO_2 (k) in the absorbent. From the comparison, it is reasonable to expect that the proposed three types of non-aqueous absorbents have valuable application potential in the field of CO_2 capture process.

We also measured the initial absorption rates of CO_2 in EHA-diglyme/triglyme/tetraglyme non-aqueous solutions at 313.2 K and 101 kPa, with the mass fractions of EHA ranging from 0.300 to 0.900, as shown in Table 6 and Fig. 9. As the absorbent concentration increases, the variation of the initial absorption rates in three non-aqueous solutions is very similar. We found when the mass fraction of EHA was 0.300, the initial absorption rate was the minimum, then increased slightly and finally tended to a fixed value (all converged to 14.85). This phenomenon shows again that the initial absorption rate is not only related to viscosity and absorbent concentration, but also to k value in Eq. (6). Combining Eq. (6) and the data presented in Tables 3 and 6, we can deduce that k value decreases monotonously with the increase of EHA concentration in a given non-aqueous solution, and k values in different non-aqueous solutions may be ranked as $k_{\text{EHA-tetraglyme}} > k_{\text{EHA-triglyme}} > k_{\text{EHA-diglyme}}$ at a given w_{EHA}.

Table 5
Viscosities (η) and initial absorption rates of CO_2 (r) of EHA-ether non-aqueous solutions and MDEA-AAIL aqueous solutions. Temperature (T) = 313.2 K. Pressure (p) = 101 kPa.

Solution	η/(mPa·s)	$r \times 1000$/(g CO_2/100 g absorbent/s)
50 wt% EHA-50 wt% diglyme	0.81	14.85
50 wt% EHA-50 wt% triglyme	1.06	14.85
50 wt% EHA-50 wt% tetraglyme	1.30	14.68
40 wt% MDEA-10 wt% [N_{1111}][Gly]	5.00 [47]	4.44
40 wt% MDEA-10 wt% [Bmim][Lys]	5.53 [48]	2.95

Table 6
Initial absorption rates of CO_2 (r) of three EHA-ether non-aqueous solutions under different mass fractions of EHA (w_{EHA}). Temperature (T) = 313.2 K. Pressure (p) = 101 kPa.

w_{EHA}	w_{ether}	$r \times 1000$/(g CO_2/100 g absorbent/s)
w_{diglyme}		
0.300	0.700	14.73
0.400	0.600	14.83
0.500	0.500	14.85
0.600	0.400	14.85
0.700	0.300	14.85
0.800	0.200	14.85
0.900	0.100	14.85
w_{triglyme}		
0.300	0.700	13.68
0.400	0.600	14.53
0.500	0.500	14.85
0.600	0.400	14.85
0.700	0.300	14.85
0.800	0.200	14.85
0.900	0.100	14.85
$w_{\text{tetraglyme}}$		
0.300	0.700	14.00
0.400	0.600	14.61
0.500	0.500	14.68
0.600	0.400	14.85
0.700	0.300	14.85
0.800	0.200	14.83
0.900	0.100	14.85

4. Conclusions

In this work, the viscosities of EHA, diglyme, triglyme, tetraglyme and EHA-diglyme/triglyme/tetraglyme non-aqueous solutions were measured and satisfactorily modeled. The effects of w_{EHA} and T on viscosity were demonstrated. The initial absorption rates of CO_2 in the EHA-ether non-aqueous solutions were measured, and the influencing factors of initial absorption rates were discussed. Our results show that:

(1) For EHA, diglyme, triglyme and tetraglyme, the viscosities decrease with increasing temperature. The viscosity of EHA is slightly higher than that of diglyme, yet significantly lower than those of triglyme and tetraglyme.
(2) For three types of EHA-ether non-aqueous solutions, the viscosities decrease with increasing temperature; for EHA-diglyme non-aqueous solution, the viscosity first decreases and then increases with increasing w_{EHA}; for EHA-triglyme and EHA-tetraglyme non-aqueous solutions, the viscosities decrease with the increase of w_{EHA}.
(3) The initial absorption rate of CO_2 is not only related to viscosity and absorbent concentration, but also to the absorption rate constant of CO_2 (k), which decreases monotonously with the increase of w_{EHA} in a given non-aqueous solution. k values for the proposed three non-aqueous solutions may be ranked as $k_{\text{EHA-tetraglyme}} > k_{\text{EHA-triglyme}} > k_{\text{EHA-diglyme}}$ at a given w_{EHA}.
(4) The proposed non-aqueous absorbents have small solution viscosities (<3 mPa·s), which is beneficial to the mass transfer of CO_2 absorption and the initial absorption rate. Thus the non-aqueous absorbents have valuable application potential in the field of CO_2 capture process.

CRediT authorship contribution statement

Kun Fu: Methodology, Software, Formal analysis, Investigation, Writing - original draft. **Pan Zhang:** Software, Investigation, Resources. **Lemeng Wang:** Software, Funding acquisition. **Xiayu Huang:** Validation, Data curation. **Dong Fu:** Conceptualization, Writing - review & editing, Supervision, Funding acquisition.

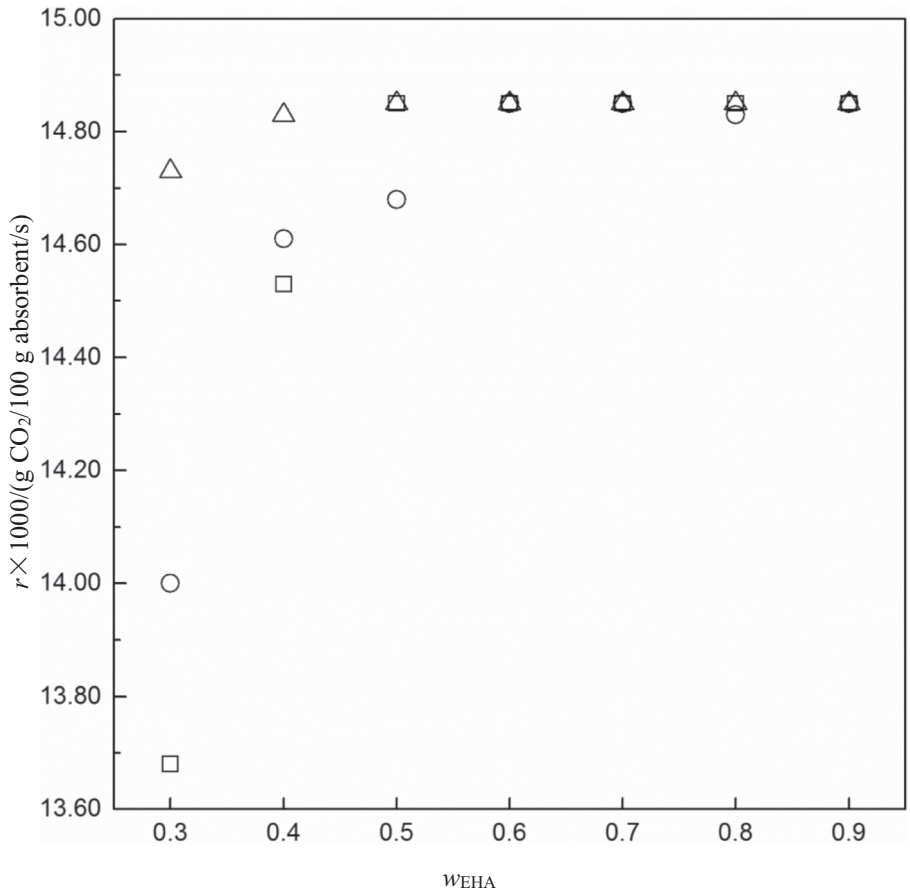

Fig. 9. w_{EHA} dependences of the initial absorption rates of CO_2 (r) in the three EHA-ether non-aqueous solutions. $T = 313.2$ K. Symbols: calculated values from this work; △EHA-diglyme; □EHA-triglyme; ◯EHA-tetraglyme.

Declaration of competing interest

The authors declare that they have no known competing financial interests or personal relationships that could have appeared to influence the work reported in this paper.

Acknowledgments

The authors appreciate the financial support by the National Natural Science Foundation of China (No. 51776072) and the Fundamental Research Funds for the Central Universities (No. 2019MS106).

Appendix A

Table A.1
Sample description.

Sample	CAS no.	Purity[a]	Water content[b]	Source
2-Ethylhexan-1-amine	104-75-6	≥99%	0.4%	Rhawn Reagent
Diglyme	111-96-6	≥99.5%	0.0036%	Rhawn Reagent
Triglyme	112-49-2	≥99%	0.03%	Acros Organics
Tetraglyme	143-24-8	≥99%	0.024%	Aladdin Reagent
N-Methyldiethanolamine	105-59-9	≥99%	0.44%	Macklin Biochemical Co., Ltd.
$[N_{1111}]$[Gly]	55378-68-2	≥98%		Cheng Jie Chemical Co., Ltd.
[Bmim][Lys]	1084610-48-9	≥98%		Cheng Jie Chemical Co., Ltd.
Carbon dioxide	124-38-9	≥99.99%		Hanjiangxue Trading Co., Ltd.
Water	7732-18-5	Electrical resistivity>15 MΩ·cm at $T = 298$ K		Heal Force ROE −100 apparatus
Certified reference materials of viscosity at moderate high temperature (viscosity standard liquids)				National Institute of Metrology, China

[a]Stated by the supplier; the purity of liquids is reported in mass percent, the purity of CO_2 is reported in volume percent.
[b]The water content is reported in mass percent. Determined by using the Karl Fischer method, as stated by the supplier.

References

[1] J.-P. Gattuso, A. Magnan, R. Billé, W.W.L. Cheung, E.L. Howes, F. Joos, D. Allemand, L. Bopp, S.R. Cooley, C.M. Eakin, Contrasting futures for ocean and society from different anthropogenic CO_2 emissions scenarios, Science 349 (2015) aac4722.

[2] M. Höök, X. Tang, Depletion of fossil fuels and anthropogenic climate change—a review, Energy Policy 52 (2013) 797–809.

[3] S.P. Singh, P.J. Hao, X. Liu, C. Wei, W.Q. Xu, N. Wei, X.C. Li, H.R. Lu, A.Y. Ku, Large-scale affordable CO_2 capture is possible by 2030, Joule 3 (2019) 2154–2164.

[4] R.N.E. Huaman, T.X. Jun, Energy related CO_2 emissions and the progress on CCS projects: a review, Renew. Sust. Energ. Rev. 31 (2014) 368–385.

[5] D. Cebrucean, V. Cebrucean, I. Ionel, CO_2 capture and storage from fossil fuel power plants, Energy Procedia 63 (2014) 18–26.

[6] D. Aaron, C. Tsouris, Separation of CO_2 from flue gas: a review, Sep. Sci. Technol. 40 (2005) 321–348.

[7] A. Hafizi, M.H. Mokari, R. Khalifeh, M. Farsi, M.R. Rahimpour, Improving the CO_2 solubility in aqueous mixture of MDEA and different polyamine promoters: the effects of primary and secondary functional groups, J. Mol. Liq. (2019) https://doi.org/10.1016/j.molliq.2019.111803.

[8] J.G. Vitillo, B. Smit, L. Gagliardi, Introduction: carbon capture and separation, Chem. Rev. 117 (2017) 9521–9523.

[9] F. Barzagli, M. Di Vaira, F. Mani, M. Peruzzini, Improved solvent formulations for efficient CO_2 absorption and low-temperature desorption, ChemSusChem 5 (2012) 1724–1731.

[10] A. Zarei, A. Hafizi, M.R. Rahimpour, S. Raeissi, Carbon dioxide absorption into aqueous potassium salt solutions of glutamine amino acid, J. Mol. Liq. (2019) https://doi.org/10.1016/j.molliq.2019.111743.

[11] S.M. Chen, S.Y. Chen, Y.C. Zhang, H.H. Chai, L. Qin, Y.T. Gong, An investigation of the role of N-methyl-diethanolamine in non-aqueous solution for CO_2 capture process using ^{13}C NMR spectroscopy, Int J Greenh Gas Control 39 (2015) 166–173.

[12] T.T. Zhang, Y.S. Yu, Z.X. Zhang, Effects of non-aqueous solvents on CO_2 absorption in monoethanolamine: ab initio calculations, Mol. Simul. 44 (2018) 815–825.

[13] H. Guo, C.X. Li, X.Q. Shi, H. Li, S.F. Shen, Nonaqueous amine-based absorbents for energy efficient CO_2 capture, Appl. Energy 239 (2019) 725–734.

[14] F. Bougie, D. Pokras, X.F. Fan, Novel non-aqueous MEA solutions for CO_2 capture, Int J Greenh Gas Control 86 (2019) 34–42.

[15] D.J. Heldebrant, P.K. Koech, V.-A. Glezakou, R. Rousseau, D. Malhotra, D.C. Cantu, Water-lean solvents for post-combustion CO_2 capture: fundamentals, uncertainties, opportunities, and outlook, Chem. Rev. 117 (2017) 9594–9624.

[16] S. Alborzi, F. Feyzi, Effect of heat stable salt bis-(2-hydroxyethyl) methylammonium formate on CO_2 absorption in aqueous methyldiethanolamine solution, J. Mol. Liq. 281 (2019) 376–384.

[17] R.R. Wanderley, Y. Yuan, G.T. Rochelle, H.K. Knuutila, CO_2 solubility and mass transfer in water-lean solvents, Chem. Eng. Sci. 202 (2019) 403–416.

[18] F. Barzagli, S. Lai, F. Mani, A new class of single-component absorbents for reversible carbon dioxide capture under mild conditions, ChemSusChem 8 (2015) 184–191.

[19] F. Barzagli, F. Mani, M. Peruzzini, A comparative study of the CO_2 absorption in some solvent-free alkanolamines and in aqueous monoethanolamine (MEA), Environ Sci Technol 50 (2016) 7239–7246.

[20] K.Y. Fu, W. Rongwong, Z.W. Liang, Y.Q. Na, R. Idem, P. Tontiwachwuthikul, Experimental analyses of mass transfer and heat transfer of post-combustion CO_2 absorption using hybrid solvent MEA-MeOH in an absorber, Chem. Eng. J. 260 (2015) 11–19.

[21] M.-K. Kang, S.-B. Jeon, J.-H. Cho, J.-S. Kim, K.-J. Oh, Characterization and comparison of the CO_2 absorption performance into aqueous, quasi-aqueous and non-aqueous MEA solutions, Int J Greenh Gas Control 63 (2017) 281–288.

[22] C. Zheng, J. Tan, Y.J. Wang, G.S. Luo, CO_2 solubility in a mixture absorption system of 2-amino-2-methyl-1-propanol with ethylene glycol, Ind. Eng. Chem. Res. 52 (2013) 12247–12252.

[23] M. Xiao, H.L. Liu, H.X. Gao, W. Olson, Z.W. Liang, CO_2 capture with hybrid absorbents of low viscosity imidazolium-based ionic liquids and amine, Appl. Energy 235 (2019) 311–319.

[24] S.M. Chen, G.P. Hu, K.H. Smith, K.A. Mumford, Y.C. Zhang, G.W. Stevens, Kinetics of CO_2 absorption in an ethylethanolamine based solution, Ind. Eng. Chem. Res. 56 (2017) 12305–12315.

[25] J. Hwang, J. Kim, H.W. Lee, J. Na, B.S. Ahn, S.D. Lee, H.S. Kim, H. Lee, U. Lee, An experimental based optimization of a novel water lean amine solvent for post combustion CO_2 capture process, Appl. Energy 248 (2019) 174–184.

[26] J. Li, C.J. You, L.F. Chen, Y.M. Ye, Z.W. Qi, K. Sundmacher, Dynamics of CO_2 absorption and desorption processes in alkanolamine with cosolvent polyethylene glycol, Ind. Eng. Chem. Res. 51 (2012) 12081–12088.

[27] H. Guo, H. Li, S.F. Shen, CO_2 capture by water-lean amino acid salts: absorption performance and mechanism, Energy Fuel 32 (2018) 6943–6954.

[28] A. Henni, P. Tontiwachwuthikul, A. Chakma, Solubilities of carbon dioxide in polyethylene glycol ethers, Can. J. Chem. Eng. 83 (2005) 358–361.

[29] D. Kodama, M. Kanakubo, M. Kokubo, S. Hashimoto, H. Nanjo, M. Kato, Density, viscosity, and solubility of carbon dioxide in glymes, Fluid Phase Equilib. 302 (2011) 103–108.

[30] H.S. Kim, J.W. Lee, L.E.E. Hyunji, Carbon dioxide absorbent, U.S. Patent Application. (2018) No. 15/761,298.

[31] Y.T. Tan, W. Nookuea, H.L. Li, E. Thorin, J.Y. Yan, Property impacts on carbon capture and storage (CCS) processes: a review, Energy Convers. Manag. 118 (2016) 204–222.

[32] A. Rahimi, A.T. Zoghi, F. Feyzi, A.H. Jalili, Experimental study of density, viscosity and equilibrium carbon dioxide solubility in some aqueous alkanolamine solutions, J. Solut. Chem. 48 (2019) 489–501.

[33] G. Murshid, H. Ghaedi, M. Ayoub, S. Garg, W. Ahmad, Experimental and correlation of viscosity and refractive index of non-aqueous system of diethanolamine (DEA) and dimethylformamide (DMF) for CO_2 capture, J. Mol. Liq. 250 (2018) 162–170.

[34] K. Fu, P. Zhang, D. Fu, Experiment and model for the viscosity of carbonated 3-(dimethylamino)propan-1-ol and 2-(ethylamino)ethanol blended aqueous solutions, J. Chem. Thermodyn. 134 (2019) 61–68.

[35] R.H. Weiland, J.C. Dingman, D.B. Cronin, G.J. Browning, Density and viscosity of some partially carbonated aqueous alkanolamine solutions and their blends, J. Chem. Eng. Data 43 (1998) 378–382.

[36] F. Barzagli, F. Mani, M. Peruzzini, Efficient CO_2 absorption and low temperature desorption with non-aqueous solvents based on 2-amino-2-methyl-1-propanol (AMP), Int J Greenh Gas Control 16 (2013) 217–223.

[37] F. Barzagli, C. Giorgi, F. Mani, M. Peruzzini, Comparative study of CO_2 capture by aqueous and nonaqueous 2-amino-2-methyl-1-propanol based absorbents carried out by ^{13}C NMR and enthalpy analysis, Ind. Eng. Chem. Res. 58 (2019) 4364–4373.

[38] K. Fu, P. Zhang, D. Fu, Absorption capacity and CO_2 removal efficiency in tray tower by using 2-(ethylamino) ethanol activated 3-(dimethylamino)propan-1-ol aqueous solution, J. Chem. Thermodyn. 139 (2019) https://doi.org/10.1016/j.jct.2019.07.004.

[39] L.M. Wang, X.F. Tian, D. Fu, X.Q. Du, J.H. Ye, Experimental investigation on CO_2 absorption capacity and viscosity for high concentrated 1-dimethylamino-2-propanol-monoethanolamine aqueous blends, J. Chem. Thermodyn. 139 (2019) https://doi.org/10.1016/j.jct.2019.07.007.

[40] G. Puxty, R. Rowland, A. Allport, Q. Yang, M. Bown, R. Burns, M. Maeder, M. Attalla, Carbon dioxide postcombustion capture: a novel screening study of the carbon dioxide absorption performance of 76 amines, Environ Sci Technol 43 (2009) 6427–6433.

[41] Natl Inst Metrol China, Certified Reference Materials of Viscosity at Moderate High Temperature, https://www.ncrm.org.cn/Repository/05197141-6993-4bbe-9b14-717eedf167ac.pdf 2018.

[42] Natl Inst Metrol China, Certified Reference Materials of Viscosity at Moderate High Temperature, https://www.ncrm.org.cn/Repository/3aee8164-5347-483f-a0a9-5271458f665f.pdf 2018.

[43] Natl Inst Metrol China, Certified Reference Materials of Viscosity at Moderate High Temperature, https://www.ncrm.org.cn/Repository/f09fc6c9-9daf-486d-8448-1feeac6b80d2.pdf 2018.

[44] M.A. Saleh, M.S. Ahmed, M.S. Islam, Viscosity and excess viscosity of dilute aqueous solutions of ethylenediamine, trimethylenediamine and N, N-dimethyltrimethylenediamine, Phys. Chem. Liq. 40 (2002) 477–490.

[45] F. Zhang, J.W. Ma, Z. Zhou, Y.T. Wu, Z.B. Zhang, Study on the absorption of carbon dioxide in high concentrated MDEA and ILs solutions, Chem. Eng. J. 181 (2012) 222–228.

[46] D.F. Othmer, M.S. Thakar, Correlating diffusion coefficient in liquids, Ind. Eng. Chem. 45 (1953) 589–593.

[47] D. Fu, P. Zhang, C.L. Mi, Effects of concentration and viscosity on the absorption of CO_2 in $[N_{1111}][Gly]$ promoted MDEA (methyldiethanolamine) aqueous solution, Energy 101 (2016) 288–295.

[48] D. Fu, P. Zhang, L.M. Wang, Absorption performance of CO_2 in high concentrated [Bmim][Lys]-MDEA aqueous solution, Energy 113 (2016) 1–8.